ACS Catalysis

Article

Alkene Synthesis by Photocatalytic, Chemoenzymatically-Compatible Dehydrodecarboxylation of Carboxylic Acids and Biomass

Vu T. Nguyen, Viet D Nguyen, Graham C. Haug, Hang T. Dang, Shengfei Jin, Zhiliang Li, Carsten Flores-Hansen, Brenda S. Benavides, Hadi D. Arman, and Oleg V. Larionov

ACS Catal., **Just Accepted Manuscript** • DOI: 10.1021/acscatal.9b02951 • Publication Date (Web): 09 Sep 2019

Alkene Synthesis by Photocatalytic, Chemoenzymatically-Compatible Dehydrodecarboxylation of Carboxylic Acids and Biomass

Vu T. Nguyen, Viet D. Nguyen, Graham C. Haug, Hang T. Dang, Shengfei Jin, Zhiliang Li, Carsten Flores-Hansen, Brenda S. Benavides, Hadi D. Arman, and Oleg V. Larionov*

Department of Chemistry, The University of Texas at San Antonio, San Antonio, Texas 78249, United States

ABSTRACT: Direct conversion of renewable biomass and bioderived chemicals to valuable synthetic intermediates for organic synthesis and materials science applications by means of mild and chemoselective catalytic methods has largely remained elusive. Development of artificial catalytic systems that are compatible with enzymatic reactions provides a synergistic solution to this enduring challenge by leveraging previously unachievable reactivity and selectivity modes. We report herein a dual catalytic dehydrodecarboxylation reaction that is enabled by a crossover of the photoinduced acridine-catalyzed O−H-HAT and cobaloxime-catalyzed C−H-HAT processes. The reaction produces a variety of alkenes from readily available carboxylic acids. The reaction can be embedded in a scalable triple-catalytic cooperative chemoenzymatic LACo process that allows for direct conversion of plant oils and biomass to long-chain terminal alkenes, precursors to bioderived polymers.

KEYWORDS acridines, alkenes, biomass, carboxylic acids, dual catalysis, photocatalysis.

1. INTRODUCTION

Alkenes are key synthetic intermediates and commodity chemicals in the industrial production of polymers, adhesives, detergents, surfactants, and plasticizers.[1] In organic synthesis, alkenes play central roles in the construction of C−C, C−O, and C−N bonds en route to active pharmaceutical ingredients, biological probes, and advanced functional materials.[2] Given the critical position of alkenes in organic chemistry, significant efforts have been directed towards development of methods of alkene synthesis. For example, Claisen and oxy-Cope rearrangements enable installation of C=C bonds in remote γ,δ- and δ,ε-positions,[3] while olefination reactions allow for the synthesis of alkenes from aldehydes and ketones.[4] Applications in polymer chemistry and industrial production of commodity chemicals rely on alkenes that are typically produced by oligomerization of coal- and petroleum-derived ethylene.[5] The process is limited to long-chain linear α-alkenes with an even number of carbon atoms. In addition, reliance on ethylene as a precursor limits applications of long-chain alkenes, e.g., in production of polyethylene-like polymers by chain-walking polymerization.[6]

Carboxylic acids are ubiquitous chemicals that are produced industrially or derived from biomass.[7] For example, long-chain fatty acids are key constituents of glycerol triesters, triglycerides that are the main components of vegetable and algal oils. Oils are renewable feedstock materials that are increasingly used as sources of bioderived chemicals and biofuel.[8] However, there are few processes that directly convert triglycerides into functionalized organic materials. Typically, isolation of fatty acids by saponification is required, before other reactions can take place. We envisioned that triglycerides can be directly converted to alkenes by a cooperative chemoenzymatic process that combines enzymatic hydrolysis of triglycerides and dehydrodecarboxylation of the intermediate fatty acids by an efficient chemical catalytic reaction. Cooperative chemoenzymatic processes merge the chemoselectivity and efficiency of enzymatic reactions with the reactivity of chemical catalysts.[9] However, enzymatic and chemical catalytic reactions typically operate under mutually incompatible conditions. For example, enzymatic reactions operate in controlled-pH aqueous solutions at near-ambient temperatures, while chemical catalytic reactions may require anhydrous conditions and elevated temperatures. Cooperative chemoenzymatic processes, therefore, remain rare and are described for a limited number of reactions. Despite these challenges, recent seminal studies on cooperative chemoenzymatic processes provide a proof of principle and an impetus for further work on this approach.[10]

Dehydrodecarboxylation of widely available and biogenic carboxylic acids can provide an efficient entry to alkenes (Figure 1). Despite the synthetic potential of this reaction, available methods of dehydrodecarboxylation suffer from drawbacks that have largely impeded its application. For example, stoichiometric amounts of toxic lead tetraacetate are required for the direct copper-catalyzed dehydrodecarboxylation.[11] Other catalytic methods allow for by-passing toxic reagents, but require prior conversion of carboxylic acids to acid chlorides or anhydrides, noble metal catalysts and high temperatures (110−400 °C).[12] Recently, several photoinduced dehydrodecarboxylation methods have been reported that enable conversion of carboxylic acids and their derivatives to alkenes at near-ambient temperatures. Glorius[13] and Shang[14] reported photoinduced dehydrodecarboxylation of *N*-hydroxy-phthalimide esters of carboxylic acids. However, these methods require prefunctionalization of carboxylic acids. On the other hand,

Ritter[15] and Tunge[16] developed photocatalytic methods for direct dehydrodecarboxylation of unprotected

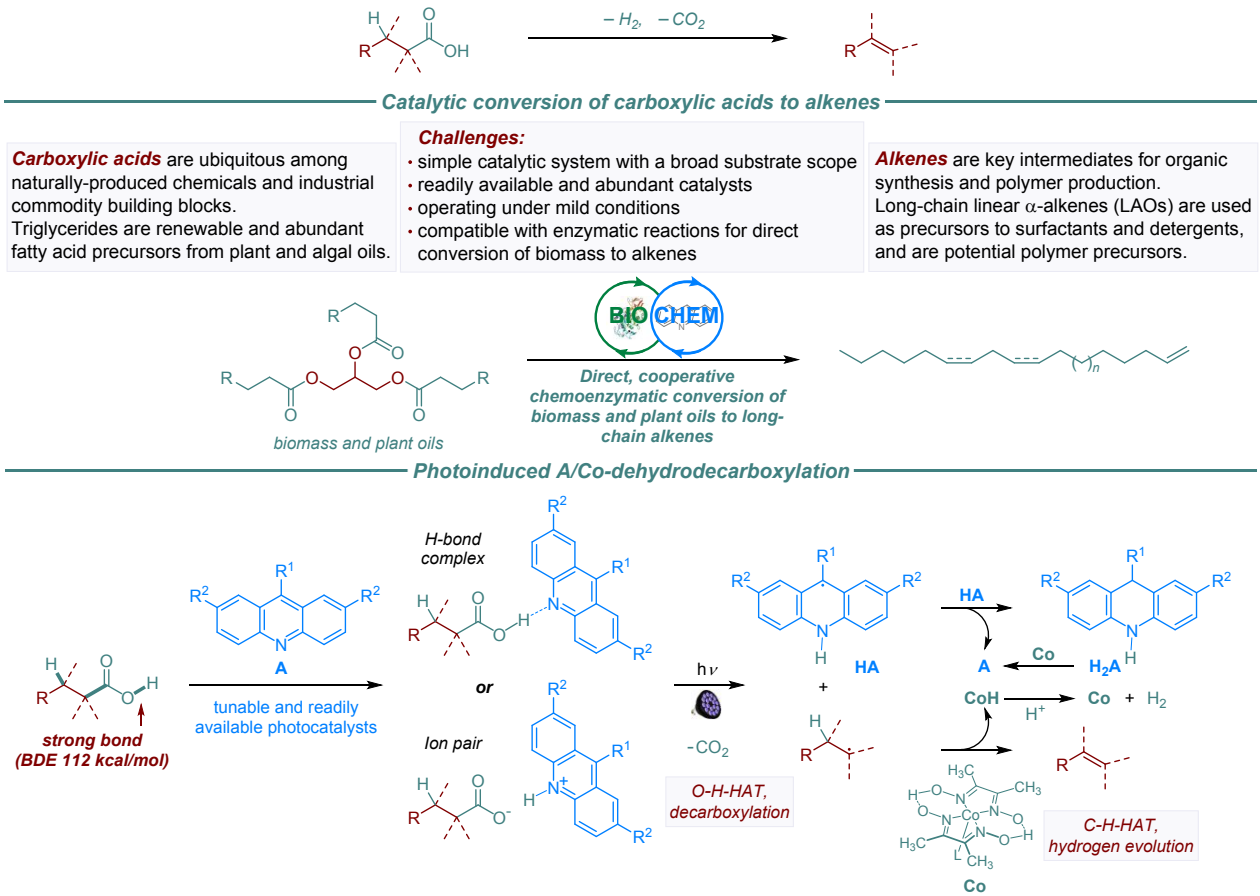

Figure 1. Catalytic dehydrodecarboxylation of carboxylic acids.

carboxylic acids with cobaloximes as a hydrogen atom transfer (HAT) catalysts.[17] Additionally, several other types of cobaloxime-catalyzed dehydrogenative coupling reactions were also recently reported.[18]

In order to develop a catalytic system for dehydrodecarboxylation that is compatible with an enzymatic reaction, we turned our attention to acridines **A** as photocatalysts for decarboxylative radical formation (Figure 1). Unsubstituted acridine is known to effect a hydrogen atom transfer from the strong O−H bond (BDE 112 kcal/mol)[19] in carboxylic acids that results in generation of alkyl radicals by decarboxylation, however, acridines have not been used as photocatalysts for synthetically important reactions.[20] The alkyl radical that is formed in the acridine-catalyzed photoinduced O−H-HAT step[21] would then undergo the α-C−H-HAT process with a cobaloxime catalyst (**Co**).[15,16,22] The cobaloxime catalyst would then enable the turnover of the acridine catalyst by dehydrogenation of dihydroacridine **H_2A** that is formed from acridine-derived radical **HA**. Although acridine is weakly basic in the ground state (pK_a = 5.6 in water), it is substantially more basic in the singlet excited state (pK_a = 10.7 in water).[23] Thus, unlike iridium and acridinium photocatalysts, acridine will not require pre-generation of carboxylate salts, since the photoinduced O−H-HAT process takes place within the acridine−carboxylic acid hydrogen bond complex or the ion pair. Furthermore, we envisioned that the photocatalytic properties of acridines could be readily fine-tuned by introducing substituents into the acridine core. These structural modifications will provide an opportunity to introduce a family of organic photocatalysts with a modus operandi that is distinct from the Ru, Ir, as well as *N*-alkyl- and arylacridinium photocatalysts that currently dominate the photocatalytic methodology.[24] Indeed, our experimental and computational studies point to a distinct mechanism of photocatalysis in the case acridines, enabling a biointerfaced triple catalytic cycle that is not attainable with Ir and acridinium photocatalysts.

2. RESULTS AND DISCUSSION

Synthetic studies. After initial optimization with unprotected deoxycholic acid (**1**), we found that the dual acridine (**A1**)/cobaloxime (**C1**)-catalyzed photoinduced dehydrodecarboxylation reaction proceeded cleanly in 88% yield in a mixture of dichloromethane and acetonitrile under LED (400 nm) irradiation in the absence of additives and activating reagents (Table 1). The reaction did not proceed in the absence of light and required both catalysts to achieve a high yield of alkene **2**. No protection was required for hydroxy groups in acid **1**, in contrast to the previously developed NHPI ester-based dehydrodecarboxylation reactions. However, the use of methanol as a co-solvent precluded formation of alkene **2**, likely because it disrupts the hydrogen bonding interaction between substrate **1** and acridine photocatalyst **A1**. Advantageously, the acridine motif can be readily accessed

by a variety of synthetic methods, including the classic Bernthsen reaction.[25] Several substituted acridines were explored as photocatalysts. Structural changes in the cobaloxime catalyst have also been studied (Figure 2). Although acridine (**A1**) and cobaloxime **C1** were found to be suitable catalysts for dehydrodecarboxylation of acid **1**, catalysts **A2-A5**, and **C2-C6** proved to be useful for achieving high yields with other substrates. In addition, the acridine catalyst loading can be reduced to 8 mol% with 9-mesitylacridine catalyst **A4**.

Table 1. Reaction conditions for dehydrodecarboxylation

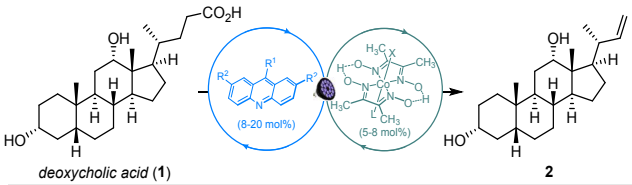

Entry	Change in the reaction conditions[a]	Yield, %[b]
1	none	88[c]
2	no irradiation	0
3	no acridine (**A1**)	0
4	no cobaloxime **C1**	0
5	methanol instead of acetonitrile	12
6	acridine **A2** instead of **A1**	75
7	acridine **A3** instead of **A1**	65
8	acridine **A4** (8 mol%) instead of **A1** and 8 mol% cobaloxime **C1**	92[c]
9	cobaloxime **C2** instead of **C1**	66
10	cobaloxime **C3** instead of **C1**	63
11	cobaloxime **C4** instead of **C1**	54

[a] Reaction conditions: acid **1** (0.3 mmol), dichloromethane/acetonitrile (2 : 1, 2.2 mL), Co catalyst **C1** (5 mol%), acridine catalyst **A1** (20 mol%), LED (λ = 400 nm), 25−27 °C, 36 h. [b] Determined by ^{1}H NMR spectroscopy with 1,4-dimethoxybenzene as an internal standard. [c] Isolated yield.

The scope of the dehydrodecarboxylation reaction was studied next (Figure 3). A variety of alkenes were produced from readily available carboxylic acid precursors. The reaction is suitable for the synthesis of allylic (β,γ) products (**3-7**) that are difficult to access by other methods, due to the ease of isomerization to the conjugated α,β-position. The synthetically challenging homoallylic (γ,δ) (**8-11**), and more remotely unsaturated (e.g., δ,ε) functionalized products **12** and **13** are also readily accessible, due to the availability of the industrially-produced precursors (e.g., adipic acid for ketone **10**). The scope of the reaction was further evaluated with substrates that are derived from natural products and active pharmaceutical ingredients. Alkenes derived from azelaic (**13**) and dihydromycophenolic (**14**) acids, as well as biotin (**15**), B-secocholestanoic acid **16**, and bile acids (**2**, **17**, and **18**) were obtained in good yields. The reaction also affords the synthetically challenging protected vinylglycine **19** from the corresponding readily available protected glutamic acid. Similarly, pinonic acid afforded the ring opening product **20** in 69% yield. Alkenes derived from chlorambucil (**21**) and sulfonamide antibiotics (**22** and **23**) were also readily produced. Products **24** and **25** derived from acids that contain the terminal alkynyl group were obtained in good yields. Carboxylic acids bearing the medicinally important fluoro and trifluoromethyl groups were also suitable substrates (**26** and **27**). Other halogen substituents were also tolerated, and alkenes bearing chloro (**28**), bromo (**26**) and iodo (**29**) groups were obtained in good yields. The acridine/cobaloxime-catalyzed dehydrodecarboxylation performed very well with a substrate featuring basic functional groups, e.g., a primary amino group and a pyridine ring (**30**), highlighting excellent functional group tolerance of the new catalytic system. Due to the recent increased interest in organoboron building blocks,[26] carboxylic acids bearing a boryl group were tested, and the products were obtained in good yields (**31** and **32**).

Given our focus on the development of the cooperative chemoenzymatic method of conversion of triglycerides to long-chain α-alkenes, we then proceeded with the investigation of the dehydrodecarboxylation of fatty acids, as well as their derivatives and analogues. Alkenes derived from stearic (**33**), palmitic (**34**), myristic (**35**), linoleic (**36**) and euricic (**37**) acids were produced in good to excellent yields. Interestingly, dehydrodecarboxylation of oleic acid allows for a one step synthesis of alkene **38** that is a pheromone of the *Oxelytrum discicolle* beetles, previously prepared in 7 steps.[27] Epoxy- and *erythro*-dichlorostearic acid-derived alkenes **39** and **40**, as well as *erythro*-aleuritic acid-derived unsaturated triol **41**, the bisacetylene-containing alkene **42** and pentadecanolide-derived alkene **43** were also readily accessible. We further explored the scope of secondary and tertiary carboxylic acids. Alkenes **44** and **45** were produced in good yields from santonic and camphoric acids.

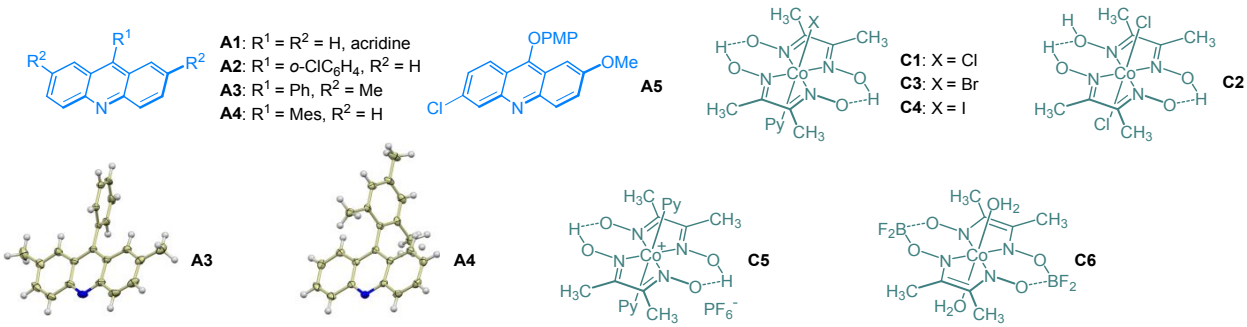

Figure 2. Acridine and cobaloxime catalysts used for dehydrodecarboxylation.

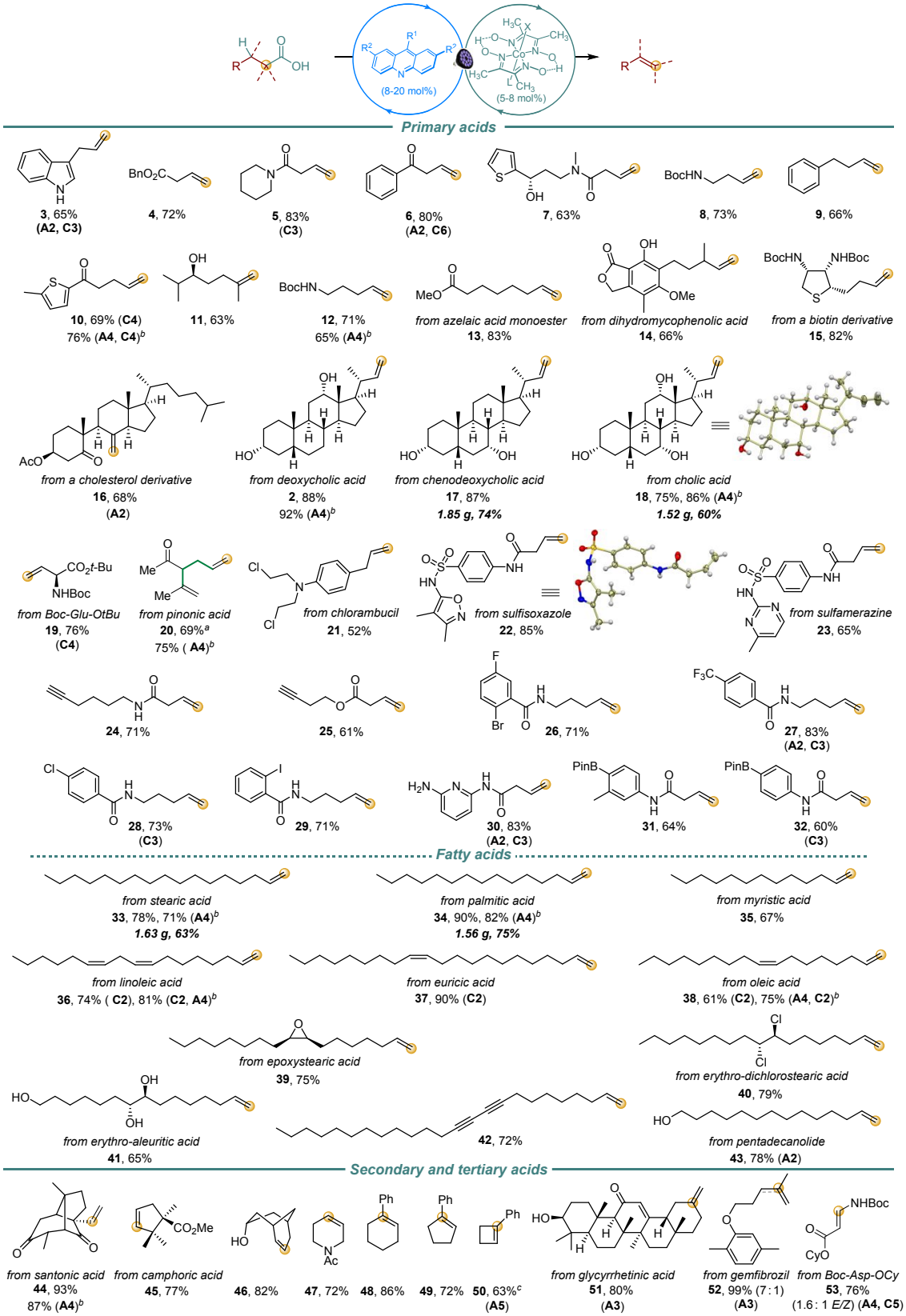

Figure 3. Scope of photoinduced dehydrodecarboxylation. Carboxylic acid (0.3 mmol), DCM/MeCN (2:1, 2.2 mL), 2×36W LED (λ = 400 nm) for 8 parallel reaction vessels, 25−27 °C, 36 h. Catalysts **A1** (20 mol%) and **C1** (5 mol%) were used unless otherwise specified. [a] Green color denotes the position of the four-membered ring in pinonic acid. [b] Catalysts **A4** (8 mol%) and **C1** (8 mol%) were used. [c] Isolated as *trans*-2-phenylcyclobutanol in 62% yield after treatment with $BH_3 \cdot THF$ followed by H_2O_2.

In addition, alkene **46** was readily prepared from the corresponding 2-adamantanone-derived carboxylic acid precursor. Tetrahydropyridine **47** was also prepared in good yield. Facile preparation of cyclic styrenes **48** and **49**

indicates that conjugated α,β-unsaturated functionalized compounds can also be prepared by the A/Co-catalyzed dehydrodecarboxylation. Remarkably, the dehydrodecarboxylation reaction proceeds efficiently even in the case of strained cyclobutene product **50** that was converted to *trans*-2-phenylcyclobutanol in 62% yield by treatment of the reaction mixture with borane and then hydrogen peroxide (see SI). This result also shows that the developed dual catalytic reaction can be readily combined with other follow-up transformations in a sequential one-pot fashion. Exocyclic dehydrodecarboxylation product **51** was favored in the case of glycyrrhetinic acid, suggesting that steric factors may be important in determining the regioselectivity of the Co-mediated C−H-HAT step. Similar preference for the terminal double bond was observed for gemfibrozil (**52**). Interestingly, the regioselectivity was higher with the present acridine-based catalytic system than in the case of the Ir/Co-catalyzed process,[15] indicating that substantial regiocontrol can be achieved in dehydrodecarboxylation of structurally complex carboxylic acids. Enamine **53** was also accessible from the corresponding aspartic acid-derived precursor.

The reaction demonstrated excellent functional group tolerance, and the oxidation-prone and reactive functional groups (e.g., unprotected indole **3**, unprotected primary and secondary alcohols **2**, **7**, **11**, **17**, **18**, thiophene **10**, sulfide **15**, aniline **21**, iodide **29**, primary amine **30**, boronic esters **31** and **32**) were not affected. The reaction also performed well with N-heterocyclic substrates (**22**, **23** and **30**), indicating that N-heterocycles do not interfere with the acridine catalysis. Other reactive functional groups, including carbonyl, amide, epoxide and internal and terminal alkynes were also tolerated. Several alkenes were prepared on gram scales (**17**, **18**, **33**, and **34**), further supporting the synthetic potential of the present catalytic dehydrodecarboxylation protocol. Although acridine (**A1**) and cobaloxime **C1** were suitable catalysts for most carboxylic acids, the reaction proceeded with diminished efficiency with some substrates. Subsequent optimization showed that the yields of alkenes can be improved by using modified acridine catalysts **A2**-**A5**, as well as cobaloximes **C2**-**C6**. (Figures 2 and 3). These results demonstrate that structural modifications in the acridine and cobaloxime catalysts can have significant effects on the efficiency and selectivity of dehydrodecarboxylation. Furthermore, in line with the result obtained for alkene **2**, 9-mesitylacridine catalyst **A4** was generally more efficient, and the acridine catalyst loading can be reduced to 8 mol%, as shown for alkenes **10**, **12**, **18**, **20**, **33**, **34**, **36**, **38**, **44**, **53**.

Development of the chemoenzymatic LACo process. We next proceeded with the development of the proposed cooperative chemoenzymatic LACo (Lipase-Acridine-Cobaloxime) process for conversion of triglycerides to long-chain alkenes. Initial experiments with stearin (glyceryl tristearate, **54**, a constituent of plant oils) as a substrate and a variety of lipases in mixtures of DCM and acetonitrile with water or respective optimal pH buffer solutions produced alkene **33** in low yields (Tables 2 and S1). Analysis of the reaction mixtures indicated that the hydrolysis was slow and incomplete. In contrast, the use of Amano lipase PS from *Burkholderia cepacia* resulted in a complete hydrolysis of triglyceride **54**, and alkene **33** was isolated in 74 % yield. A lower yield was observed with water instead of a pH 7 buffer solution, while very little product was formed in the absence of the lipase or the aqueous buffer solution. Remarkably, the acridine/cobaloxime catalytic system proved to be the only catalytic system that enables the triple catalytic conversion of triglycerides directly to long-chain alkenes, as no product was observed with iridium-[15] and acridinium[16] salt-based photocatalytic systems (Table 2, entries 9−10 and Table S1, entries 19−21). The lipase can be reused without deterioration in yields. The LACo process can be carried out on a gram scale (Figure 4) and can be extended to other triglycerides, for example glycerol tripalmitate (palmitin, 83% yield). Furthermore, the reaction can be carried out with hydrogenated sunflower, corn, canola, and soybean oils, producing alkenes **55** in 62−83% yields. Additionally, sunflower, canola, corn, and soybean oils can be directly converted to alkenes **55** in good yields, indicating that the LACo process can be used

Table 2. Reaction conditions for cooperative chemoenzymatic LACo process

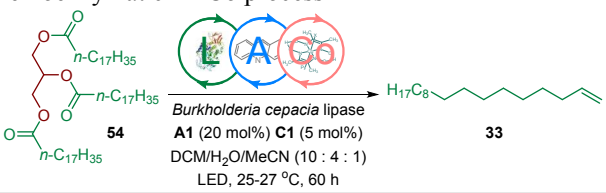

Entry	Change in reaction conditions [a]	Yield, % [b]
1	none	74[c]
2	lipase from *Candida rugosa*	10
3	lipase from *Penicillium camemberti*	9
4	lipase from *Pseudomonas fluorescens*	33
5	lipase from *Mucor javanicus*	20
6	water instead of pH 7 buffer	61
7	no pH 7 buffer	11
8	no lipase	8
9	$Ir[dF(CF_3)ppy]_2(dtbpy)PF_6$ (1 mol%) instead of **A1**	0[d,e]
10	$[Mes\text{-}Acr\text{-}Me]^+ClO_4^-$ (5 mol%) instead of **A1**	0[e,f]

[a] Reaction conditions: triglyceride **54** (0.1 mmol), dichloromethane/acetonitrile (10 : 1, 1.6 mL), aqueous solution (0.7 mL), Co catalyst **C1** (5 mol% per stearyl residue), acridine catalyst **A1** (20 mol% per stearyl residue), lipase from *Burkholderia cepacia*, 27 °C, LED (λ = 400 nm), 60 h. [b] Determined by ^1H NMR spectroscopy with 1,4-dimethoxybenzene as an internal standard. [c] Isolated yield. [d] In the presence of Cs_2CO_3 (20 mol%). [e] With blue LEDs. [f] The cobaloxime catalyst (3 mol%) was preactivated with sodium

triacetoxyborohydride as described previously, and the reaction was carried out for 36 h in MeOH/H_2O.[16a]

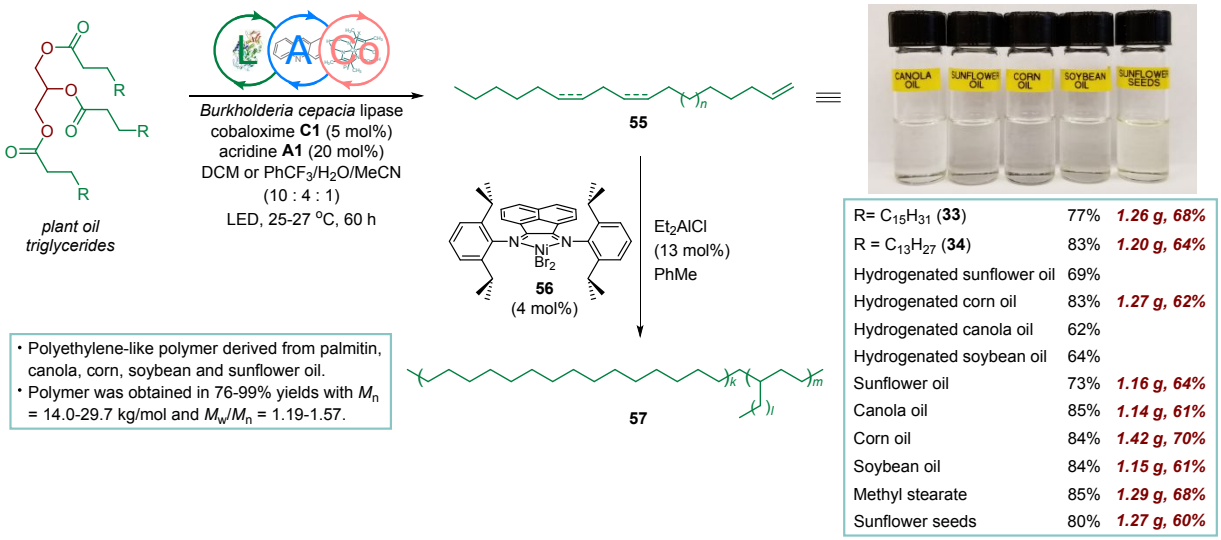

Figure 4. Cooperative chemoenzymatic LACo process and polymerization of plant oil-derived alkenes.

for production of long-chain alkenes from a variety of plant-derived feedstock materials.

GC-MS analysis of alkenes **55** produced from sunflower oil revealed presence of individual alkenes derived from stearic (**33**), palmitic (**34**), linoleic (**36**), and oleic (**38**) acids. The cooperative chemoenzymatic reaction can also be successfully used with methyl esters of fatty acids (MEFAs), − industrially important plant and algal oil-derived chemicals, − as exemplified by conversion of methyl stearate to alkene **33** in 85% yield. Remarkably, the LACo process can be directly applied to unrefined biomass. For example, sunflower seeds (52% oil content) were used for production of alkenes **55** that were isolated in good yield (Figure 4). This result demonstrates the potential of the developed process for direct conversion of unrefined biomass to valuable synthetic intermediates. Moreover, the LACo process can be readily carried out on gram scales with the plant oils tested, and with unrefined biomass. As with the dehydrodecarboxylation of carboxylic acids, the LACo process can also be carried out successfully with reduced loading of acridine catalyst **A4** (8 mol%), producing alkenes **55** in 78 and 73% yields from canola and soybean oils, respectively.

Plant oil-derived alkenes **55** obtained in the LACo process can find use as surfactants and detergents that are currently produced by oligomerization of petroleum- and coal-derived ethylene. In addition, plant oil-derived chemicals have recently attracted significant attention as renewable feedstock monomers for polymer production.[8] We, therefore, tested feasibility of conversion of plant oils to polymers produced from long-chain alkenes by a sequence of the LACo process and a chain-walking polymerization[6] with nickel catalyst **56** and diethylaluminum chloride as a co-catalyst. Gratifyingly, both palmitin-derived alkene **34** and the alkenes produced from hydrogenated canola, corn, soybean and sunflower oils were readily converted to polyethylene-like polymer **57** in good yields (76-99%) with molecular weight (M_n) in the range of 14.0−29.7 kg/mol and narrow molecular weight distribution (M_w/M_n = 1.19−1.57) (see SI for further details).

Mechanistic studies. Cobaloximes have been studied extensively as catalysts for photocatalytic hydrogen evolution.[28] Mechanistic investigations demonstrated involvement of Co^{II} and Co^{I} cobaloxime species that are responsible for the absorptions in the 400−470 nm and 560−620 nm ranges in the visible spectra of the hydrogen evolution reactions.[29] Additionally, involvement of the putative cobaloxime hydride species $Co^{III}H$ as a key intermediate in the hydrogen evolution reaction (HER), possibly in equilibrium with other isomeric forms, was proposed.[30] Cobaloximes are also used as catalysts in radical polymerization. 17-Electron Co^{II} cobaloximes exhibit radical behavior and are known to react with alkyl radicals via β-hydrogen abstraction (producing alkenes) and cross-termination (producing Co(III) alkylcobaloximes) at diffusion-controlled rates (>10^9–10^{10} L/mol·s).[31] The diffusion-controlled rates of cobaloxime/alkyl radical reactions combined with persistence of Co^{II} cobaloximes enable the persistent radical (Ingold-Fischer) effect[32] that results in the predominant reaction of alkyl radicals with cobaloxime,[33] outcompeting other possible pathways for alkyl radical sequestration, e.g., diffusion-controlled self-termination or a much slower (e.g., <10^2 L/mol·s)[34] hydrogen atom transfer from solvent. The β-hydrogen abstraction pathway is at the heart of the mechanism of the catalytic chain transfer (CCT) polymerization, while the reversible cross-termination that produces alkylcobaloxime intermediates allows for an efficient end-capping in the living radical polymerization (LRP).[31,35] With this mechanistic information in mind, we turned our attention to investigation of the mechanism of the dual catalytic dehydrodecarboxylation.

Our optimization experiments indicated that both acridine and cobaloxime catalysts were essential to effect dehydrodecarboxylation, and alkene products were not

observed, when either of the catalysts was omitted (Table 1, entries 2 and 3). Given the possibility of an exchange of the chloride in cobaloxime **C1** with carboxylate arising from deprotonation of the carboxylic acid by acridine, and the precedented thermal decarboxylation of cobalt(III) carboxylates,[36] we interrogated a mechanistic scenario that involves the anion metathesis of chloride with carboxylate in cobaloxime catalyst **C1**. This step is followed by photoactivation of the cobaloxime carboxylate intermediate (See Fig S1, decarboxylation-on-cobaloxime mechanism). Subsequent photoinduced single-electron transfer from carboxylate to cobaloxime results in decarboxylation and formation of the alkyl radical and $\mathbf{Co^{II}}$ intermediate that further produce the alkene product and cobalt intermediate $\mathbf{Co^{III}H}$. Given the ancillary role of acridine as a proton shuttle in this mechanism, it was expected to be readily replaceable with other bases. Accordingly, reactions were carried out with palmitic acid, catalytic cobaloxime **C1**, and various organic and inorganic bases in place of acridine (pyridine, triethylamine, diisopropylethylamine, K_2CO_3, Cs_2CO_3) in catalytic (20 mol%) and stoichiometric quantities (Table S2). In addition, solutions of cobaloxime **C1** with sodium and potassium palmitate were subjected to the irradiation. Cobaloxime **C1** was also pretreated with silver palmitate with subsequent exposure to the LED light after filtration. Furthermore, reactions were performed in the presence of TEMPO (2 equiv.) to trap any radical intermediates (Table S2, entries 18−21). In no case was formation of alkene **34** or any other products observed. Additionally, no carbon dioxide was detected by GC in the reactor headspace, when acridine was replaced by pyridine (Table S3, entry 5). We also tested the hypothesis that decarboxylation occurs at cobaloxime after an energy transfer from acridine by replacing acridine with eosin Y (Table S2, entries 22−23). Eosin Y is known to effect a highly efficient energy transfer to cobaloxime **C1** at diffusion-controlled rates.[37] As with earlier experiments, no decarboxylation products were observed in the absence or in the presence of TEMPO. Taken together, these experiments rule out the decarboxylation-on-cobaloxime mechanism.

In order to test the mechanistic proposal that involves photoinduced hydrogen atom transfer from carboxylic acid to the acridine catalyst (Figure 1, decarboxylation-on-acridine mechanism), palmitic acid was reacted with TEMPO in the presence of acridines **A1-A4** as photocatalysts (Figure 5 and Table S4). The product of cross-termination of the alkyl radical with TEMPO **58** was formed in 68% yield with **A1** in the absence of cobaloxime (Figure 5A), and carbon dioxide was detected by GC in the reactor headspace (Table S3, entry 6), validating the decarboxylation-on-acridine mechanistic proposal. Similar reactivity was observed for other acridine catalysts (Figure 5A and Table S4), with acridine **A4** providing cross-termination product **58** in the highest yield (77% in trifluorotoluene). Addition of TEMPO (2 equiv.) to the **A4**/**C1**-catalyzed dehydrodecarboxylation reaction of palmitic acid resulted in suppression of formation of alkene **34**, indicating that TEMPO disrupts the dual catalytic system via competitive trapping of the alkyl radical (Figure 5A). In order to rule out the possibility that TEMPO shuts down dehydrodecarboxylation by reacting with cobaloxime **C1**, we carried out additional experiments with varied initial loadings of TEMPO (Figure 5B). The yield of alkene **34** decreased monotonically in response to the increased initial loading of TEMPO, while the yield of product **58** grew proportionately (lines a and b, respectively, in Figure 5B). The reaction with TEMPO was

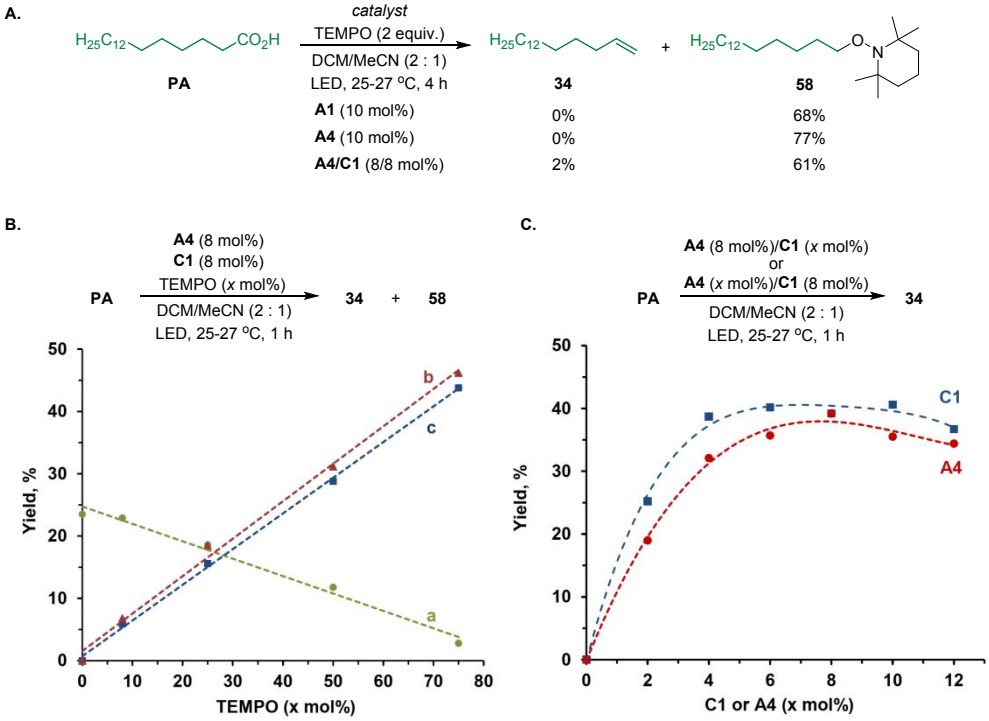

Figure 5. Radical trapping experiments with TEMPO and the influence of varied initial catalyst loading on the photoinduced dehydrodecarboxylation reaction. (A) Reaction of palmitic acid (**PA**) with TEMPO in the absence and in the presence of catalyst **C1**. (B)

Influence of the initial loading of TEMPO on the **A4**/**C1**-photocatalyzed dehydrodecarboxylation of palmitic acid (**PA**) after 1 h. (**a**) —●— : yield of alkene **34** in the presence of varied amounts of TEMPO; (**b**) —▲— : yield of product **58** in the absence of catalyst **C1**; (**c**) —■— : yield of product **58** in the presence of catalyst **C1**. (C) Influence of the initial loading of catalyst **C1** (—■—) or **A4** (—●—) on the **A4**/**C1**-photocatalyzed dehydrodecarboxylation of palmitic acid (**PA**) after 1 h.

substantially faster than the dehydrodecarboxylation, as evidenced by the small effect of added catalyst **C1** on the yield of TEMPO product **58** (lines b and c). On the other hand, the monotonic decrease in the yield of alkene **34** with increasing loading of TEMPO indicates that TEMPO does not shut down the dehydrodecarboxylation by deactivating catalyst **C1**. Collectively, data presented in Figure 5A,B demonstrate that TEMPO acts as a competitive inhibitor of the alkyl radical capture by the cobaloxime-derived reactive species after the acridine-catalyzed decarboxylation. Furthermore, experiments with varied catalyst **C1** loadings showed that the optimal **C1** loading was achieved in the range of 6−10 mol% with 8 mol% **A4**, while further increase in the **C1** loading did not improve the reaction performance (Figure 5C). Similar observations were made in experiments with varied acridine **A4** loadings, wherein the optimal loading of **A4** was achieved at 8 mol% (Figure 5C). These results indicate that a kinetic saturation is achieved with respect to the carryover of the alkyl radical from the acridine catalytic cycle to the cobaloxime catalytic cycle.

In order to further support the conclusion that the alkyl radical that is produced in the acridine catalytic cycle is then intercepted by a Co(II) cobaloxime intermediate, the dehydrodecarboxylation reaction was performed in the presence of stoichiometric amounts of Co(II) cobaloxime **C6**, and the corresponding transient alkylcobaloxime intermediate (see below for further discussion) was observed by means of electrospray high resolution mass spectroscopy (Figure S2B).

Additionally, Stern-Volmer fluorescence quenching experiments showed that acetic acid was a competent quencher for fluorescent acridine catalyst **A5** (but not for the cobaloxime catalyst, Figures S5, S9), indicating that the reaction is likely initiated by quenching the acridine with carboxylic acids.

Although amines are typically sufficiently basic to deprotonate carboxylic acids and form carboxylate salts in aqueous solutions (e.g., pK_{BH^+} = 10.6 for *n*-butylamine,[38] and pK_a = 4.8 for acetic acid[39] in water), the relative acidity relationship *is inverted* in less polar solvents (e.g., pK_{BH^+} = 18.3 for *n*-butylamine, and pK_a = 21.6 for acetic acid in acetonitrile),[38] making formation of carboxylate salts thermodynamically unfavorable. Instead, formation of hydrogen-bonded heteroconjugated species (e.g., RH_2N−HOAc, heteroconjugation constant K = 2089) is observed.[38] Attenuation of amine basicity leads to a further decrease in interactions between amines and carboxylic acids in solvents of lower polarity.

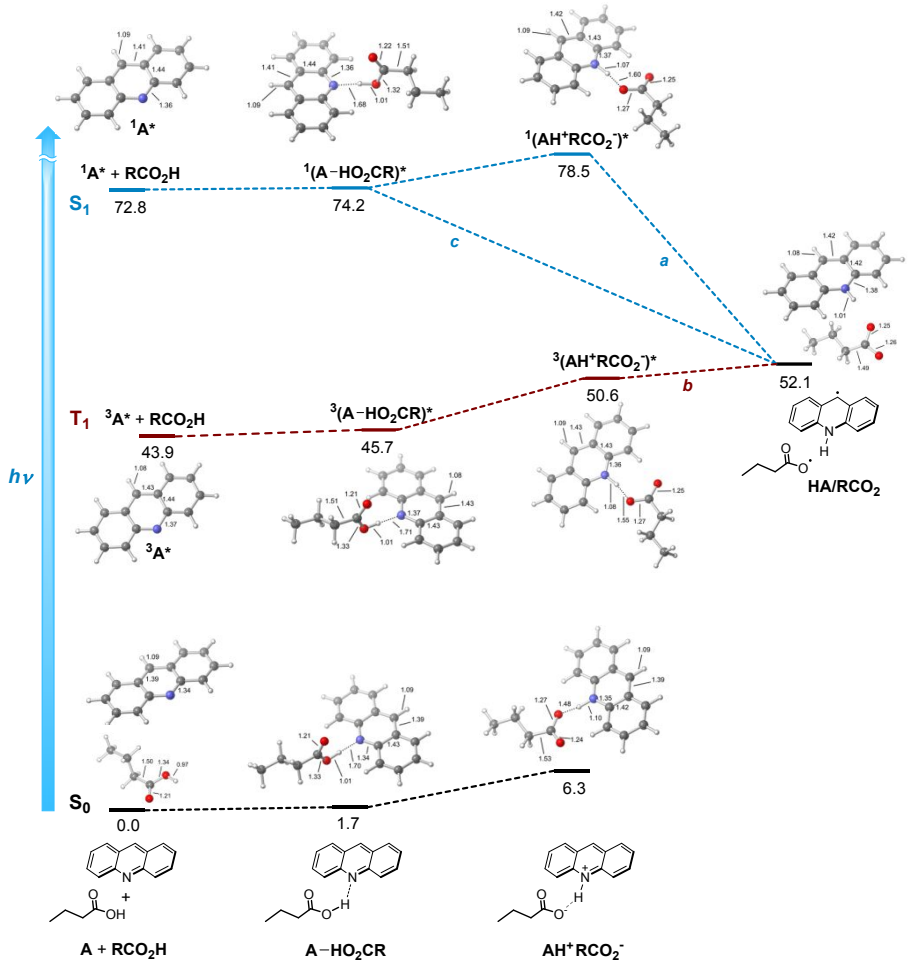

Figure 6. Computational studies (ωB97X-D/6-311-G**/SMD(DCM), Δ*G*, kcal/mol) of the photoinduced PCET in the acridine−carboxylic acid system. In figures 6−8, the blue arrow depicts vertical excitation that is followed by vibrational relaxation, as well as internal conversion and intersystem crossing to lower energy singlet and triplet excited states.

For example, lower heteroconjugation constant (K = 98) is observed for the less basic 4-methylimidazole (pK_{BH}^{+} = 12.2 in MeCN).[38] Given the comparable basicity of acridine (pK_{BH}^{+} = 12.7 in MeCN[40]) and the presence of the less polar cosolvent (ε = 9.1, $E_T(30)$ = 40.7 kcal/mol for dichloromethane, ε = 37.5, $E_T(30)$ = 45.6 kcal/mol for acetonitrile),[41] the acridine–carboxylic acid system is expected to be dominated by the uncomplexed amine and acid, as well as hydrogen-bonded conjugated species, with negligible involvement of acridinium carboxylate. Indeed, absorption spectra of a solution of acridine in the presence of acetic acid showed a weak bathochromic shift (Figures S11−S16) that is evident in the difference absorption spectrum (Figure S15) and correlates with the appearance of a light yellow color of a previously colorless acridine solution upon addition of acetic acid (Figure S17). However, the acridine–acetic acid system spectra did not show a characteristic broad shoulder with a λ_{max} in the 400–430 nm range that is known to be observed for acridinium salts and that can be clearly seen in the absorption spectra of acridine in the presence of trifluoroacetic acid (pK_a = 12.7 in MeCN,[39] Figures S18−S22) and triflic acid TfOH (pK_a = 2.6 in MeCN,[39] Figures S23−S27) and is particularly evident in the respective difference absorption spectra (Figures S19 and S24). For comparison, no changes were observed in the absorption spectra of cobaloxime **C1** upon addition of acetic acid (Figures S28−S33).

DFT computational studies of the acridine−butyric acid system at the (U)ωB97X-D/6-311+G**/SMD(DCM) level of theory corroborate these observations (Figure 6). While acridinium butyrate (**$AH^+O_2CR^-$**) is substantially (6.3 kcal/mol) less stable than the uncomplexed reactants, pointing to the very low concentration of the acridinium carboxylate in the reaction mixture, heteroconjugated hydrogen-bonded complex **A−HO_2CR** is close in thermodynamic stability to the reactants (1.7 kcal/mol). Although the concentration of acridinium ions is negligible in the ground state, it can be formed by a proton transfer (PT) in the singlet or triplet excited state of **A−HO_2CR** complex, or via the protonation of the excited acridine. These processes are thermodynamically unfavorable (see Figure 6), however, given the energy attained in the intersystem crossing and internal conversion after the vertical excitation, they may take place in the lowest singlet and triplet states. Subsequent electron transfer (ET) from carboxylate to acridinium may produce radical pair **HA/RCO_2** (i.e., pathways ***a*** and ***b*** in Figure 6). However, the process is thermodynamically unfavorable in the triplet state, potentially making the stepwise triplet PT-ET a less

unlikely pathway for the formation of radical pair **HA/RCO$_2$**, while the singlet excited state PT-ET may not be competitive with an efficient HAT process from the singlet excited **A−HO$_2$CR** complex (*c*, see below). Our experimental evidence supports this consideration. Protonation is substantially more favorable in the more polar solvent methanol, and concentrations of ammonium carboxylate salts are much higher for amine−carboxylic acid systems in methanol (e.g., pK_a = 8.02 for 4-methylimidazole and 7.26 for AcOH in MeOH, formation of the salt is thermodynamically favorable).[38] However, the dehydrodecarboxylation (Table 1, entry 5) and the reaction with TEMPO (Table S4, entry 7) do not take place in methanol, despite the higher concentration of

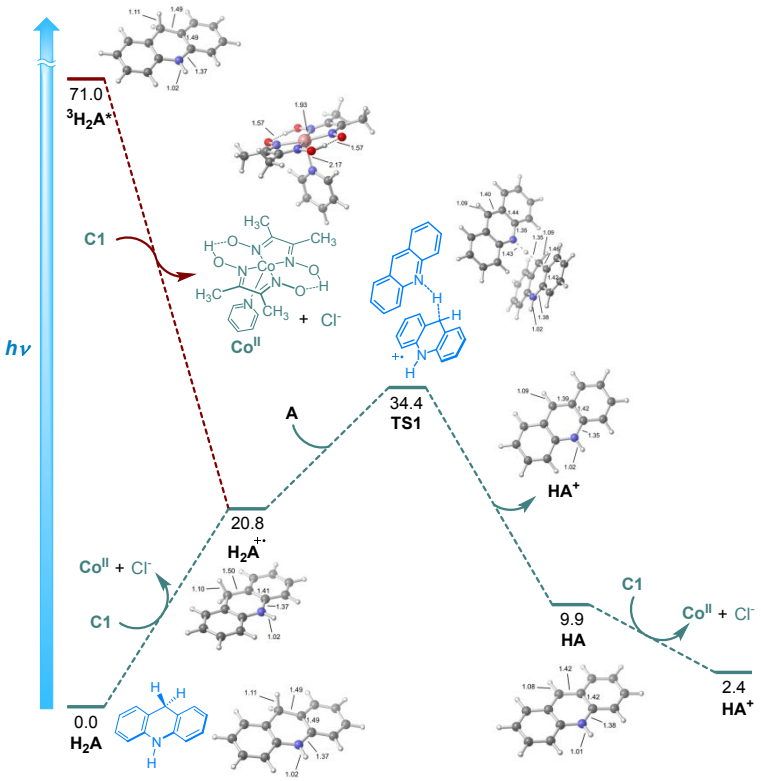

Figure 7. Computed energy profile (ωB97X-D/6-311-G**/SMD(DCM), Δ*G*, kcal/mol) for the reduction of Co(III) cobaloxime catalysts -induced acridine−carboxylic acid system.

the acridinium ion in this more polar solvent (Δ*G* = 1.5 kcal/mol in methanol, see Figure S42, cf. Δ*G* = 6.3 kcal/mol in dichloromethane). This result also highlights the importance of formation of heteroconjugated hydrogen-bonded complex **A−HO$_2$CR**, since heteroconjugation is known to be disrupted in methanol.[38] In order to further test the involvement of acridinium carboxylate ion pair and the importance of hydrogen-bonded complex **A−HO$_2$CR**, the reaction with TEMPO was carried out under the standard conditions with *N*-methylacridinium palmitate obtained in the anion exchange reaction with silver palmitate and *N*-methylacridinium iodide, as well as with *N*-methylacridinium iodide or tetrafluoroborate in the presence of palmitic acid with and without pyridine as a base or with tetrabutylammonium palmitate instead of palmitic acid (Table S4, entries 9−14). *N*-Methylacridinium ion can form ion pairs with carboxylates, but cannot produce a hydrogen-bonded complex of type **A−HO$_2$CR**, while exhibiting an absorption spectrum in the visible range that is nearly identical to that of acridinium (cf. Figures S18 and S41). Significantly, in all cases, less than 4% of TEMPO product **58** or no reaction was observed, further supporting the conclusion that the acridinium carboxylate ion pair of **AH$^+$O$_2$CR$^-$** type is not involved in the acridine catalysis.

Taken together, these experimental and computational results are in line with the general observation that preassociation and hydrogen-bonding are crucial features of proton-coupled electron transfer (PCET) processes.[42] The importance of formation of heteroconjugated hydrogen-bonded complex **A−HO$_2$CR** in the photoinduced PCET en route to radical pair **HA/RCO$_2$** can be understood in the context of the short lifetime of the singlet excited state of uncomplexed acridine (τ = 0.045 ns)[43] that may be insufficient to engage in a productive bimolecular PCET process. Since the lowest singlet excited state of acridine is of the n→π* type,[44] the photoinduced PCET process (pathway ***c***) can be described as a hydrogen atom transfer.[42] The lowest triplet excited state of acridine, on the other hand, is of the π→π* type,[44] and the corresponding concerted PCET process en route to radical pair **HA/RCO$_2$** will be a concerted electron proton transfer.[42] The conversion to the radical pair **HA/RCO$_2$** from the lowest triplet of **A−HO$_2$CR** is endergonic, potentially reducing the efficiency of the triplet pathway. This computational conclusion is corroborated by the prior experimental observations that oxygen, − a very efficient triplet quencher

for acridine and acridinium salts ($E_s(^1\Delta_g)$ = 22.5 kcal/mol, quantum yield for quenching of triplet acridine by oxygen ϕ_Δ = 0.83)[45] – does not have a detrimental effect on photoinduced reactions of acridine, and the molecular reactions of excited acridine are dominated by the singlet excited state.[46] Indeed, the acridine **A4**-catalyzed reaction with TEMPO was not significantly affected by performing it in the atmosphere of oxygen (Table S4, entry 8), indicating that triplet states are unlikely to be significantly involved in the decarboxylation pathway. Collectively, the experimental and computational results point to the singlet excited state of the heteroconjugated hydrogen-bonded complex **A−HO$_2$CR** as the key intermediate in the dehydrodecarboxylation.

Acridinyl radical **HA** that is produced in the photoinduced PCET step can directly reduce cobaloxime **C1**, in parallel to the known single-electron reduction of **C1** by 2-hydroxypropyl radical.[47] Indeed, the reduction of **C1** by **HA** was found to be thermodynamically favorable (ΔG = –7.5 kcal/mol, Figure 7), providing a pathway for the regeneration of the acridine catalyst (via conversion of acridinium **HA**$^+$ to acridine **A** in the HER pathway, see below) and formation of intermediate **Co^{II}** that plays a key role in the interception of alkyl radicals en route to alkenes. This reduction pathway can be especially important for the production of **Co^{II}** from Co(III) cobaloximes in the initial stages of the catalytic process.

In addition to the direct reduction of **C1** to **Co^{II}**, acridinyl radical **HA** can undergo disproportionation to dihydroacridine **H$_2$A** and acridine catalyst **A** that is known to proceed with near diffusion-controlled rates (>10^8 L/mol·s).[48] Indeed, analysis of the reaction mixture by NMR spectroscopy points to substantial accumulation of dihydroacridine **H$_2$A** (~6 mol % after 20 min). Hypothesizing that the regeneration of acridine catalyst **A** takes place by a cobaloxime-induced oxidation of dihydroacridine **H$_2$A**, we studied the behavior of dihydroacridine (**H$_2$A**) in the presence of cobaloximes **C1**. While no reaction was observed in the

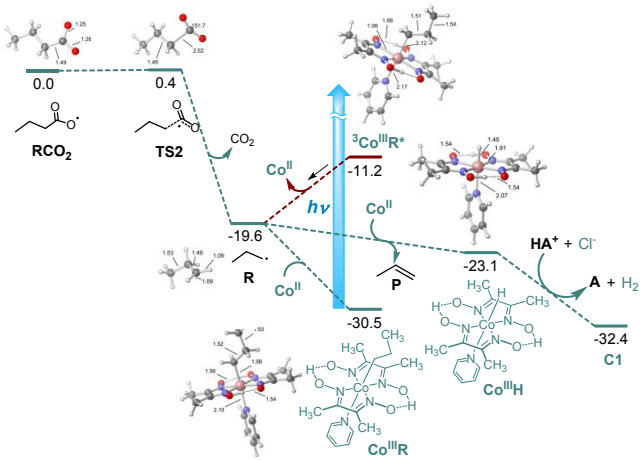

Figure 8. Computed energy profile (ωB97X-D/6-311-G**/SDD(Co)/SMD(DCM), ΔG, kcal/mol) for the dehydrodecarboxylation reaction.

absence of light, dihydroacridine (**H$_2$A**) underwent photoinduced oxidation with cobaloxime **C1** (Figure S43). Negligible amount (<1%) of hydrogen was produced in the reaction, as evidenced by GC studies of the reactor overhead space (Table S3), excluding substantial involvement of the hydrogen evolution reaction and hydridocobaloxime intermediates. Further studies showed that cobaloxime **C1** is an efficient quencher of fluorescence of dihydroacridine (Figure S7). On the other hand, no fluorescence quenching was observed for the fluorescent cobaloxime **C2** with a nonfluorescent amine (diisopropylethylamine, Figure S10. Thus, the reaction may be initiated by an electron transfer from the photoexcited dihydroacridine **H$_2$A** to the cobaloxime catalyst, resulting in formation of Co(II) cobaloxime **Co^{II}**. DFT computational studies (Figure 7) show that the step is exergonic from the triplet excited state (but endergonic in the ground state, in line with the experimental observation of no dark reaction). Radical cation **H$_2$A$^{+\cdot}$** can then undergo a proton transfer (e.g., with acridine in the dehydrodecarboxylation reaction) to give acridinyl radical **HA** in an exergonic step (ΔG = –9.3 kcal/mol, $\Delta G^{\neq}$ = 13.7 kcal/mol), thus providing a pathway for regeneration of **HA** that can subsequently reduce **C1** to **Co^{II}**, as described above. Co(II) cobaloximes are common intermediates in photoinduced hydrogen evolution reactions (HER),[28] and their formation is readily deduced from the reaction mixture absorption spectra, due to the appearance of a strong absorption band in the 400−470 nm range.[29] However, the acridinium ion also absorbs in the same range (Figures S18−S27), and the strong absorption band in this range that is indeed observed in the spectra of the photoinduced reaction of cobaloxime **C1** with dihydroacridine may be due to the presence of both products (Figures S34, S35). The presence of **Co^{II}** in the reaction mixture was, therefore, further confirmed experimentally by ESI-HRMS and EPR studies (Figure S3).

The persistent radical behavior of Co(II) cobaloximes is known to enable an efficient cross-termination with alkyl radicals (persistent radical effect) that under thermal conditions produces Co(III) alkylcobaloximes. The selectivities for cross-termination with cobaloximes over self-termination of alkyl radicals can reach 10^5:1,[33] and the reaction occurs at diffusion-controlled rates, effectively suppressing side reactions. Due to the weakness of the Co−C bond (21−29 kcal/mol),[49] the reaction can be readily reversed both thermally and photochemically. Photoinduced cleavage of alkylcobaloximes is known to produce alkyl radicals and Co(II) cobaloximes that further undergo β-hydrogen atom transfer to give alkenes.[31,33,50] Our experimental studies show that decarboxylation takes place in the acridine catalytic cycle, with the acridine catalyst turnover being assisted by the cobaloxime catalysis. Kinetic experiments with TEMPO and varied amounts of **A4** and **C1** catalysts (Figure 5) support the carryover of the alkyl radical from the acridine catalytic cycle to cobaloxime. Furthermore, as in the case of the photoinduced reaction of dihydroacridine with **C1**, ESI-HRMS and EPR studies of the dehydrodecarboxylation reaction mixture (Figure S2A,C) demonstrated presence of cobaloxime **Co^{II}** that is known to play a key role in the

interception of the alkyl radical and its engagement in a β-hydrogen abstraction en route to alkenes via photoreversible formation of alkylcobaloximes.[51] As discussed above, ESI-HRMS studies of the dehydrodecarboxylation reaction mixture also confirmed the presence of the alkylcobaloxime intermediate (Figure S2B), further supporting the mechanism that involves acridine-catalyzed generation of the alkyl radical and its subsequent trapping by **Co^{II}**. In order to further probe the involvement of alkylcobaloximes in the acridine/cobaloxime-catalyzed dehydrodecarboxylation, *n*-octylcobaloxime was used as a catalyst, and the kinetic behavior of the reaction was found to be comparable to the **C1**-catalyzed reaction (Figure S44), indicating that alkylcobaloximes can be involved in the cobaloxime catalytic cycle. *n*-Octylcobaloxime was found to undergo rapid decomposition to give 1-octene under the LED irradiation (87% consumption in 10 min, Figure S45). These results indicate that, if formed prior to β-hydrogen abstraction en route to the alkene, alkylcobaloximes undergo rapid photoinduced homolysis. Halpern's prior kinetic studies of photodecomposition of alkylcobaloximes[51] determined that the new absorption band in the 410−470 nm range is due to the formation of **Co^{II}** cobaloxime intermediate that is produced upon photoinitiated decomposition of hydridocobaloxime **Co^{III}H**.

The absorption band in the 400−470 nm range was also observed for the reaction mixture of the dehydrodecarboxylation reaction (Figures S36, S37), although acridinium can also contribute to the absorption. Hence, presence of **Co^{II}** was additionally confirmed by EPR and ESI-HRMS, as discussed above. Finally, hydrogen was detected by GC in the reactor overhead space, along with carbon dioxide (produced in the acridine catalytic cycle) (Table S3),

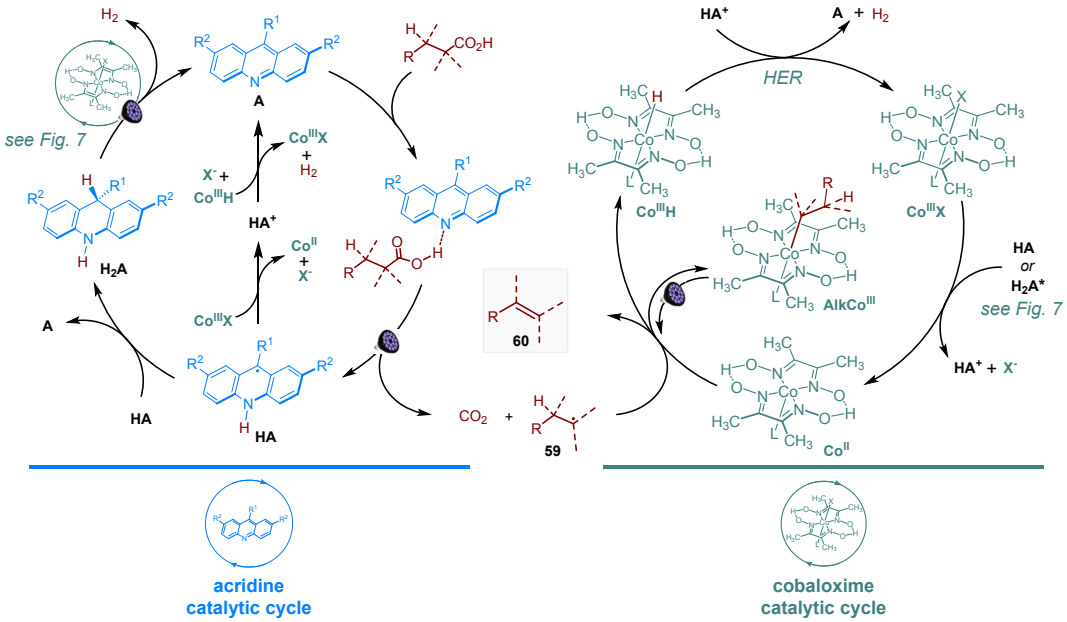

Figure 9. Mechanism of the acridine/cobaloxime dual catalytic photoinduced dehydrodecarboxylation reaction.

supporting involvement of the hydrogen evolution reaction (HER) in the cobaloxime catalytic cycle.

In order to gain further insight into the mechanism of the dehydrodecarboxylation, DFT computational studies for the cobaloxime-catalyzed conversion of acyloxy radical **R** produced in the acridine catalytic cycle were performed (Figure 8). Decarboxylation of radical **R** was found to be exergonic (ΔG = −19.6 kcal/mol) and occurring in a near barrierless fashion ($\Delta G^{\neq}$ = 0.4 kcal/mol), in line with prior experimental observations.[52] The β-hydrogen abstraction from alkyl radical **R** by **Co^{II}** also proceeds exergonically (ΔG = –3.5 kcal/mol), affording hydridocobaloxime **Co^{III}H** and the alkene product.[53] Alkyl radical **R** and **Co^{II}** can also produce alkylcobaloximes **Co^{III}R** that can undergo photoinduced homolysis from the triplet state. The reaction between **Co^{III}H** and acridinium **HA^{+}** produces hydrogen and regenerates catalyst **C1** in a hydrogen evolution reaction (HER) in a net exergonic step (ΔG = –9.3 kcal/mol). The mechanism of HER with proton sources, including protonated amines, was recently studied in detail computationally and experimentally, and involvement of ligand-protonated intermediates was proposed in addition to homolytic and heterolytic pathways.[30,54] Taken together, the mechanism of the dehydrodecarboxylation reaction can be described as a dual catalytic process. The acridine catalytic cycle enables the photoinduced decarboxylation and feeds alkyl radical **59** into the cobaloxime catalytic cycle that effects β-hydrogen abstraction en route to alkene product **60** directly or via the photoreversible formation of alkylcobaloxime **AlkCo^{III}**. The ensuing hydrogen evolution reaction from **Co^{III}H** completes the cobaloxime catalytic cycle (Figure 9). The complex catalytic network also includes the cobaloxime-catalyzed turnover of the acridine catalyst via oxidation of acridinyl radical **HA** and dihydroacridine **H$_2$A**.

Given the general sensitivity and mutual incompatibility of biocatalyzed and chemically-catalyzed reactions, it is

remarkable that acridine catalysts enable the facile interfacing of the biocatalyzed ester hydrolysis and dehydrodecarboxylation in a triple catalytic process. It is especially remarkable in light of the failure of the iridium and acridinium photocatalysts to effect the biointerfaced triple catalytic process. The key to the success of the acridine system may lie in the directed (via hydrogen bonding) HAT-type character of the acyloxy radical generation event, as opposed to electron transfer that may require additives (e.g., bases to generate carboxylate anions) or may cause deleterious side reactions and off-cycle photocatalyst quenching.

3. CONCLUSION

In this paper, we describe a dual catalytic system for dehydrodecarboxylation of carboxylic acids that enabled development of a cooperative chemoenzymatic synthesis of alkenes from triglycerides and directly from unrefined biomass. The bioderived alkenes were readily converted to polymers, demonstrating the synthetic potential of the cooperative chemoenzymatic LACo process. We also showed that simple and inexpensive acridine photocatalysts can be efficiently used for photoinduced hydrogen atom transfer in a dual catalytic process. The scalable acridine/cobaloxime-catalyzed dehydrodecarboxylation reaction exhibits a broad substrate scope and functional group tolerance.

AUTHOR INFORMATION

Corresponding Author

*E-mail: oleg.larionov@utsa.edu

ASSOCIATED CONTENT

The Supporting Information is available free of charge on the ACS Publications website at DOI: 10.1021/. Experimental procedures, characterization and X-Ray crystallographic analysis data, NMR spectra, and details of the computational investigations.

ACKNOWLEDGMENT

Financial support by the Welch Foundation (AX-1788), the NSF (CHE-1455061 and CHE-1625963), and the Brown Foundation is gratefully acknowledged. We thank Profs. Donald Kurtz and Kirk Schanze (UTSA) for assistance with GC, fluorescence and GPC measurements. The authors acknowledge the Texas Advanced Computing Center (TACC) at the University of Texas at Austin for providing computational resources.

CONFLICT OF INTEREST

The UTSA has filed a provisional patent application for the process described in this publication.

REFERENCES

(1) (a) Domski, G. J.; Rose, J. M.; Coates, G. W.; Bolig, A. D.; Brookhart, M. Living Alkene Polymerization: New Methods for The Precision Synthesis of Polyolefins. *Prog. Polym. Sci.* **2007**, *32*, 30–92. (b) Myers, D. *Surfactant science and technology*; John Wiley & Sons: Hoboken, NJ, 2005. (c) Wypych, G. *Plasticizer types. Handbook of plasticizers*; ChemTec Publishing: Ontario, Canada, 2017. (d) Olah, G. A.; Molnár, Á. *Hydrocarbon chemistry*; John Wiley & Sons: Hoboken, NJ, 2003.

(2) (a) Coombs, J. R.; Morken, J. P. Catalytic Enantioselective Functionalization of Unactivated Terminal Alkenes. *Angew. Chem. Int. Ed.* **2016**, *55*, 2636–2649. (b) McDonald, R. I.; Liu, G.; Stahl, S. S. Palladium(II)-Catalyzed Alkene Functionalization via Nucleopalladation: Stereochemical Pathways and Enantioselective Catalytic Applications. *Chem. Rev.* **2011**, *111*, 2981–3019. (c) Wang, X.; Studer, A. Iodine(III) Reagents in Radical Chemistry. *Acc. Chem. Res.* **2017**, *50*, 1712–1724. (d) Landry, M. L.; Burns, N. Z. Catalytic Enantioselective Dihalogenation in Total Synthesis. *Acc. Chem. Res.* **2018**, *51*, 1260–1271. (e) Green, S. A.; Vásquez-Céspedes, S.; Shenvi, R. A. Iron–Nickel Dual-Catalysis: A New Engine for Olefin Functionalization and the Formation of Quaternary Centers. *J. Am. Chem. Soc.* **2018**, *140*, 11317–11324. (f) Wu, X.; Riedel, J.; Dong, V. M. Transforming Olefins into γ,δ-Unsaturated Nitriles through Copper Catalysis. *Angew. Chem. Int. Ed.* **2017**, *56*, 11589–11593. (g) Margrey, K. A.; Nicewicz, D. A. A General Approach to Catalytic Alkene Anti-Markovnikov Hydrofunctionalization Reactions via Acridinium Photoredox Catalysis. *Acc. Chem. Res.* **2016**, *49*, 1997–2006. (h) Grela, K. *Olefin Metathesis: Theory and Practice;* John Wiley & Sons: Hoboken, NJ, 2014. (i) Nicolaou, K. C.; Bulger, P. G.; Sarlah, D. Metathesis Reactions in Total Synthesis. *Angew. Chem. Int. Ed.* **2005**, *44*, 4490–4527. (j) Michaudel, Q.; Kottisch, V.; Fors, B. P. Cationic Polymerization: from Photoinitiation to Photocontrol. *Angew. Chem. Int. Ed.* **2017**, *56*, 9670–9679.

(3) (a) Martín Castro, A. M. Claisen Rearrangement over the Past Nine Decades. *Chem. Rev.* **2004**, *104*, 2939–3002. (b) Ilardi, E. A.; Stivala, C. E.; Zakarian, A. [3,3]-Sigmatropic Rearrangements: Recent Applications in the Total Synthesis of Natural Products. *Chem. Soc. Rev.* **2009**, *38*, 3133–3148. (c) Jones, A. C.; May, J. A.; Sarpong, R.; Stoltz, B. M. Toward a Symphony of Reactivity: Cascades Involving Catalysis and Sigmatropic Rearrangements. *Angew. Chem. Int. Ed.* **2014**, *53*, 2556–2591.

(4) Takeda, T. *Modern carbonyl olefination: Methods and applications*; John Wiley & Sons: Hoboken, NJ, 2006.

(5) (a) McGuinness, D. S. Olefin Oligomerization via Metallacycles: Dimerization, Trimerization, Tetramerization, and Beyond. *Chem. Rev.* **2010**, *111*, 2321–2341. (b) Gollwitzer, A.; Dietel, T.; Kretschmer, W. P.; Kempe, R. A Broadly Tunable Synthesis of Linear α-Olefins. *Nat. Commun.* **2017**, *8*, 1226.

(6) (a) Johnson, L. K.; Killian, C. M.; Brookhart, M. New Pd(II)- and Ni(II)-Based Catalysts for Polymerization of Ethylene and. α-Olefins. *J. Am. Chem. Soc.* **1995**, *117*, 6414–6415. (b) Vaidya, T.; Klimovica, K.; LaPointe, A. M.; Keresztes, I.; Lobkovsky, E. B.; Daugulis, O.; Coates, G. W. Secondary Alkene Insertion and Precision Chain-Walking: A New Route to Semicrystalline "Polyethylene" From α-Olefins by Combining Two Rare Catalytic Events. *J. Am. Chem. Soc.* **2014**, *136*, 7213–7216.

(7) Goossen, L. J.; Rodriguez, N.; Gooßen, K. Carboxylic Acids as Substrates in Homogeneous Catalysis. *Angew. Chem. Int. Ed.* **2008**, *47*, 3100–3120.

(8) (a) Kerenkan, A. E.; Béland, F.; Do, T. O. Chemically Catalyzed Oxidative Cleavage of Unsaturated Fatty Acids and Their Derivatives into Valuable Products for Industrial Applications: A Review and Perspective. *Catal. Sci. Technol.* **2016**, *6*, 971–987. (b) Wu, L.; Moteki, T.; Gokhale, A. A.; Flaherty, D. W.; Toste, F. D. Production of Fuels and Chemicals from Biomass: Condensation Reactions and Beyond. *Chem* **2016,** *1*, 32−58. (c) Hess, S. K.; Lepetit, B, Kroth, P. G.; Mecking. S. Production of Chemicals from Microalgae Lipids – Status and Perspectives. *Eur. J. Lipid Sci. Technol.* **2018**, *120*, 1700152.

(9) Rudroff, F.; Mihovilovic, M. D.; Gröger, H.; Snajdrova, R.; Iding, H.; Bornscheuer, U. T. Opportunities and ChallengesfFor Combining Chemo- and Biocatalysis. *Nature Catal.* **2018**, *1*, 12–22.

(10) (a) Burda, E.; Hummel, W.; Gröger, H. Modular Chemoenzymatic One-Pot Syntheses in Aqueous Media: Combination of a Palladium-Catalyzed Cross-Coupling with an Asymmetric Biotransformation. *Angew. Chem. Int. Ed.* **2008**, *47*, 9551-9554. (b) Denard, C. A.; Huang, H.; Bartlett, M. J.; Lu, L.; Tan,

Y.; Zhao, H.; Hartwig, J. F. Cooperative Tandem Catalysis by an Organometallic Complex and a Metalloenzyme. *Angew. Chem. Int. Ed.* **2014**, *53*, 465–469. (c) Denard, C. A.; Bartlett, M. J.; Wang, Y.; Lu, L.; Hartwig, J. F.; Zhao, H. Development of a One-Pot Tandem Reaction Combining Ruthenium-Catalyzed Alkene Metathesis and Enantioselective Enzymatic Oxidation to Produce Aryl Epoxides. *ACS Catal.* **2015**, *5*, 3817–3822. (d) Latham, J.; Henry, J. M.; Sharif, H. H.; Menon, B. R.; Shepherd, S. A.; Greaney, M. F.; Micklefield, J. Integrated Catalysis Opens New Arylation Pathways via Regiodivergent Enzymatic C–H Activation. *Nat. Commun.* **2016**, *7*, 11873. (e) Litman, Z. C.; Wang, Y.; Zhao, H.; Hartwig, J. F. Cooperative Asymmetric Reactions Combining Photocatalysis and Enzymatic Catalysis. *Nature* **2018**, *560*, 355. (f) Cosgrove, S. C.; Hussain, S.; Turner, N. J.; Marsden, S. P. Synergistic Chemo/Biocatalytic Synthesis of Alkaloidal Tetrahydroquinolines. *ACS Catal.* **2018**, *8*, 5570–5573.

(11) Bacha, J. D.; Kochi, J. K. Alkenes from Acids by Oxidative Decarboxylation. *Tetrahedron* **1968**, *24*, 2215–2226.

(12) (a) Liu, Y.; Kim, K. E.; Herbert, M. B.; Fedorov, A.; Grubbs, R. H.; Stoltz, B. M. Palladium-Catalyzed Decarbonylative Dehydration of Fatty Acids for the Production of Linear Alpha Olefins. *Adv. Synth. Catal.* **2014**, *356*, 130–136. (b) Miranda, M. O.; Pietrangelo, A.; Hillmyer, M. A.; Tolman, W. B. Catalytic Decarbonylation of Biomass-Derived Carboxylic Acids as Efficient Route to Commodity Monomers. *Green Chem.* **2012**, *14*, 490–494. (c) Chatterjee, A.; Hopen Eliasson, S. H.; Törnroos, K. W.; Jensen, V. R. **2016**, Palladium Precatalysts for Decarbonylative Dehydration of Fatty Acids to Linear α-Olefins. *ACS Catal.* **2012**, *6*, 7784–7789. (d) Liu, Y.; Virgil, S. C.; Grubbs, R. H.; Stoltz, B. M. Palladium-Catalyzed Decarbonylative Dehydration for the Synthesis of α-Vinyl Carbonyl Compounds and Total Synthesis of (−)-Aspewentins A, B, and C. *Angew. Chem. Int. Ed.* **2015**, *54*, 11800–11803. (e) Chatterjee, A.; Eliasson, S. H. H.; Jensen, V. R. Selective Production of Linear α-Olefins via Catalytic Deoxygenation of Fatty Acids and Derivatives. *Catal. Sci. Technol.* **2018**, *8*, 1487–1499. (f) Zhang, X.; Jordan, F.; Szostak, M. Transition-Metal-Catalyzed Decarbonylation of Carboxylic Acids to Olefins: Exploiting Acyl C–O Activation for the Production of High Value Products. *Org. Chem. Front.* **2018**, *5*, 2515–2521. (g) Shang, R., Leu, L. *Sci. China Chem.* **2011**, *54*, 1670–1687.

(13) Tlahuext-Aca, A.; Candish, L.; Garza-Sanchez, R. A.; Glorius, F. Decarboxylative Olefination of Activated Aliphatic Acids Enabled by Dual Organophotoredox/Copper Catalysis. *ACS Catal.* **2018**, *8*, 1715–1719.

(14) Cheng, W. M.; Shang, R.; Fu, Y. Irradiation-Induced Palladium-Catalyzed Decarboxylative Desaturation Enabled by a Dual Ligand System. *Nature Commun.* **2018**, *9*, 5215.

(15) Sun, X.; Chen, J.; Ritter, T. Catalytic Dehydrogenative Decarboxyolefination of Carboxylic Acids. *Nat. Chem.* **2018**, *10*, 1229–1233.

(16) (a) Cartwright, K. C.; Tunge, J. A. Decarboxylative Elimination of *N*-Acyl Amino Acids via Photoredox/Cobalt Dual Catalysis. *ACS Catal.* **2018**, *8*, 11801–11806. (b) Cartwright, K. C.; Lang, S. B.; Tunge, J. A. Photoinduced Kochi Decarboxylative Elimination for the Synthesis of Enamides and Enecarbamates from *N*-Acyl Amino Acids. *J. Org. Chem.* **2019**, *84*, 2933−2940.

(17) Green, S. A.; Crossley, S. W. M.; Matos, J. L. M.; Vásquez-Céspedes, S.; Shevick, S. L.; Shenvi, R. A. The High Chemofidelity of Metal-Catalyzed Hydrogen Atom Transfer. *Acc. Chem. Res.* **2018**, *51*, 2628−2640.

(18) (a) Meng, Q. -Y.; Zhong, J. -J.; Liu, Q.; Gao, X. -W.; Zhang, H. -H.; Lei, T.; Li, Z.-J.; Feng, K.; Chen, B.; Tung, C. -H.; Wu, L. -Z. A Cascade Cross-Coupling Hydrogen Evolution Reaction by Visible Light Catalysis. *J. Am. Chem. Soc.* **2013**, *135*, 19052–19055. (b) Zhang, G.; Liu, C.; Yi, H.; Meng, Q.; Bian, C.; Chen, H.; Jian, J.X.; Wu, L. Z.; Lei, A. External Oxidant-Free Oxidative Cross-Coupling: a Photoredox Cobalt-Catalyzed Aromatic C–H Thiolation for Constructing C–S Bonds. *J. Am. Chem. Soc.* **2015**, *137*, 9273–9280. (c) Wu, C. -J.; Meng, Q. -Y.; Lei, T.; Zhong, J. -J.; Liu, W. -Q.; Zhao, L. -M.; Li, Z. -J.; Chen, B.; Tung, C. -H.; Wu, L. -Z. An Oxidant-Free Strategy for Indole Synthesis via Intramolecular C-C Bond Construction under Visible Light Irradiation: Cross-Coupling Hydrogen Evolution Reaction. *ACS Catal.* **2016**, *6*, 4635−4639 (d) Hu, X.; Zhang, G.; Bu, F.; Luo, X.; Yi, K.; Zhang, H.; Lei, A. Photoinduced Oxidative Activation of Electron-Rich Arenes: Alkenylation with H_2 Evolution under External Oxidant-Free Conditions. *Chem. Sci.* **2018**, *9*, 1521−1526. (e) Tang, S.; Zeng, L; Lei, A. Oxidative R_1–H/R_2–H Cross-Coupling with Hydrogen Evolution. *J. Am. Chem. Soc.* **2018**, *140*, 13128−13135. (f) Wang, H.; Gao, X.; Lv, Z.; Abdelilah, T.; Lei, A. Recent Advances in Oxidative R_1−H/R_2−H Cross-Coupling with Hydrogen Evolution via Photo-/Electrochemistry. *Chem. Rev.* **2019**, *119*, 6769−6787.

(19) Blanksby, S. J.; Ellison, G. B. Bond Dissociation Energies of Organic Molecules. *Acc. Chem. Res.* **2003**, *36*, 255–263.

(20) Noyori, R.; Kato, M.; Kawanisi, M.; Nozaki, H. Photochemical Reaction of Benzopyridines with Alkanoic Acids Novel Reductive Alkylation of Acridine, Quinoline and Isoquinoline under Decarboxylation. *Tetrahedron* **1969**, *25*, 1125−1136.

(21) Liu, X.; Karsili, T. N.; Sobolewski, A. L.; Domcke, W. Photocatalytic Water Splitting with the Acridine Chromophore: A Computational Study. *J. Phys. Chem. B.* **2015**, *119*, 10664−10672.

(22) (a) Inokuchi, T.; Tsuji, M.; Kawafuchi, H.; Torii, S. Indirect electroreduction of 2-Alkyl-2-(bromomethyl)cycloalkanones with Cobaloxime to Form 3-Alkyl-2-alkenones via 1,2-Acyl Migration. *J. Org. Chem.* **1991**, *56*, 5945–5948. (b) West, J. G.; Huang, D.; Sorensen, E. J. Acceptorless Dehydrogenation of Small Molecules Through Cooperative Base Metal Catalysis. *Nat. Commun.* **2015**, *6*, 10093. (c) Abrams, D. J.; West, J. G.; Sorensen, E. J. Toward a Mild Dehydroformylation Using Base-Metal Catalysis. *Chem. Sci.* **2017**, *8*, 1954–1959. (d) Cao, H.; Jiang, H.; Feng, H.; Kwan, J. M. C.; Liu, X.; Wu, J. Photo-induced Decarboxylative Heck-Type Coupling of Unactivated Aliphatic Acids and Terminal Alkenes in the Absence of Sacrificial Hydrogen Acceptors. *J. Am. Chem. Soc.* **2018**, *140*, 16360–16367.

(23) (a) Pines, E.; Huppert, D.; Gutman, M.; Nachliel, N.; Fishman, M. The *p*OH Jump: Determination of Deprotonation Rates of Water by 6-Methoxyquinoline and Acridine. *J. Phys. Chem.* **1986**, *90*, 6366–6370. (b) Ireland, J. F.; Wyatt, P. A. H. Acid-Base Properties of Electronically Excited States of Organic Molecules. *Adv. Phys. Org. Chem.* **1976**, *12*, 131–221.

(24) (a) Prier, C. K.; Rankic, D. A.; MacMillan, D. W. Visible Light Photoredox Catalysis with Transition Metal Complexes: Applications in Organic Synthesis. *Chem. Rev.* **2013**, *113*, 5322–5363. (b) Romero, N. A.; Nicewicz, D. A. Organic photoredox catalysis. *Chem. Rev.* **2016**, *116*, 10075–10166. (c) Griffin, J. D.; Zeller, M. A.; Nicewicz, D. A. Hydrodecarboxylation of Carboxylic and Malonic Acid Derivatives via Organic Photoredox Catalysis: Substrate Scope and Mechanistic Insight. *J. Am. Chem. Soc.* **2015**, *137*, 11340−11348. (d) Narayanam, J. M.; Stephenson, C. R. Visible Light Photoredox Catalysis: Applications in Organic Synthesis. *Chem. Soc. Rev.* **2011**, *40*, 102–113. (e) Yoon, T. P.; Ischay, M. A.; Du, J. Visible Light Photocatalysis as a Greener Approach to Photochemical Synthesis. *Nat. Chem.* **2010**, *2*, 527. For an alternative photocatalytic system based on Ph_3P/NaI, see: (f) Fu, M.-C.; Shang, R.; Zhao, B.; Wang, B.; Fu, Y. Photocatalytic Decarboxylative Alkylations Mediated by Triphenylphosphine and Sodium Iodide. *Science* **2019**, *363*, 1429−1434.

(25) Schmidt, A.; Liu, M. Recent Advances in the Chemistry of Acridines. *Adv. Heterocycl. Chem.* **2015**, *115*, 287–353.

(26) (a) Hall, D. G. *Boronic Acids*; Wiley-VCH: Weinheim, Germany, 2011. (b) Nguyen, V. D.; Nguyen, V. T.; Jin, S.; Dang, H. T.; Larionov, O. V. Organoboron Chemistry Comes to Light: Recent Advances in Photoinduced Synthetic Approaches to Organoboron Compounds. *Tetrahedron* **2019**, *75*, 584–602.

(27) Fockink, D. H.; Mise, K. M.; Zarbin, P. H. Male-produced Sex Pheromone of the Carrion Beetles, *Oxelytrum discicolle* and Its Attraction to Food Sources. *J. Chem. Ecol.* **2013**, *39*, 1056–1065.

(28) (a) Dempsey, J. L.; Brunschwig, B. S.; Winkler, J. R.; Gray, H. B. Hydrogen Evolution Catalyzed by Cobaloximes. *Acc. Chem. Res.* **2009**, *42*, 1995–2004. (b) Dalle, K. E.; Warnan, J.; Leung, J. J.;

Reuillard, B.; Karmel, I. S.; Reisner, E. Electro-and Solar-driven Fuel Synthesis with First Row Transition Metal Complexes. *Chem. Rev.* **2019**, *119*, 2752–2875.

(29) (a) Lazarides, T.; McCormick, T.; Du, P.; Luo, G.; Lindley, B.; Eisenberg, R. Making Hydrogen from Water Using a Homogeneous System without Noble Metals. *J. Am. Chem. Soc.* **2009**, *131*, 9192–9194. (b) Du, P.; Schneider, J.; Luo, G.; Brennessel, W. W.; Eisenberg, R. Visible Light-driven Hydrogen Production from Aqueous Protons Catalyzed by Molecular Cobaloxime Catalysts. *Inorg. Chem.* **2009**, *48*, 4952–4962.

(30) Estes, D. P.; Grills, D. C.; Norton, J. R. The Reaction of Cobaloximes with Hydrogen: Products and Thermodynamics. *J. Am. Chem. Soc.* **2014**, *136*, 17362–17365.

(31) (a) Halpern, J.; Ng, F. T.; Rempel, G. L. Metal-alkyl Bond Dissociation Energies in Organocobalt Compounds Related to Vitamin B12 Coenzymes. *J. Am. Chem. Soc.* **1979**, *101*, 7124–7126. (b) Gridnev, A. A.; Ittel, S. D. Catalytic Chain Transfer in Free-Radical Polymerizations. *Chem. Rev.* **2001**, *101*, 3611–3660.

(32) (a) Fischer, H. Unusual Selectivities of Radical Reactions by Internal Suppression of Fast Modes. *J. Am. Chem. Soc.* **1986**, *108*, 3925–3927. (b) Fischer, H. The Persistent Radical Effect: A Principle for Selective Radical Reactions and Living Radical Polymerizations. *Chem. Rev.* **2001**, *101*, 3581–3610.

(33) (a) Branchaud, B. P.; Yu, G. X. An Example of the Persistent Radical Effect in Cobaloxime-mediated Radical Alkyl-alkenyl Cross Coupling. *Organometallics* **1993**, *12*, 4262–4264. (b) Daikh, B. E.; Finke, R. G. The Persistent Radical Effect: A Prototype Example of Extreme, 105 to 1, Product Selectivity in a Free-radical Reaction Involving Persistent. Co^{ii}[macrocycle] and Alkyl Free Radicals. *J. Am. Chem. Soc.* **1992**, *114*, 2938–2943. (c) Studer, A. The Persistent Radical Effect in Organic Synthesis. *Chem. Eur. J.* **2001**, *7*, 1159–1164.

(34) Hendry, D. G.; Mill, T.; Piszkiewicz, L.; Howard, J. A.; Eigenmann, H. K. A Critical Review of H-Atom Transfer in the Liquid Phase: Chlorine Atom, Alkyl, Trichloromethyl, Alkoxy, and Alkylperoxy Radicals. *J. Phys. Chem. Ref. Data* **1974**, *3*, 937–978.

(35) Demarteau, J.; Debuigne, A.; Detrembleur, C. Organocobalt Complexes as Sources of Carbon-Centered Radicals for Organic and Polymer Chemistries. *Chem. Rev.* **2019**, *119*, 6906−6955.

(36) Lande, S. S.; Kochi, J. K. Formation and Oxidation of Alkyl Radicals by Cobalt(III) Complexes. *J. Am. Chem. Soc.* **1968**, *90*, 5196–5207.

(37) Wang, J.; Li, C.; Zhou, Q.; Wang, W.; Hou, Y.; Zhang, B.; Wang, X. Enhanced Photocatalytic Hydrogen Production by Introducing the Carboxylic Acid Group into Cobaloxime Catalysts. *Dalton Trans.* **2015**, *44*, 17704–17711.

(38) Kozak, A.; Czaja, M.; Chmurzyński, L. Investigations of (Acid+Base) Equilibria in Systems Modelling Interactions Occurring in Biomolecules. *J. Chem. Thermodynamics*. **2006**, *38*, 599–605.

(39) Kütt, A.; Leito, I.; Kaljurand, I.; Sooväli, L.; Vlasov, V. M.; Yagupolskii, L. M.; Koppel, I. A. A Comprehensive Self-consistent Spectrophotometric Acidity Scale of Neutral Brønsted Acids in Acetonitrile. *J. Org. Chem.* **2006**, *71*, 2829–2838.

(40) Lõkov, M.; Tshepelevitsh, S.; Heering, A.; Plieger, P. G.; Vianello, R.; Leito, I. On the Basicity of Conjugated Nitrogen Heterocycles in Different Media. *Eur. J. Org. Chem.* **2017**, *30*, 4475–4489.

(41) (a) Reichardt, C. Solvatochromic Dyes as Solvent Polarity Indicators. *Chem. Rev.* **1994**, *94*, 2319–2358. (b) Smallwood, I. *Handbook of Organic Solvent Properties*; Amold, London, 1996; pp 137, 289.

(42) Weinberg, D. R.; Gagliardi, C. J.; Hull, J. F.; Murphy, C. F.; Kent, C. A.; Westlake, B. C.; Paul, A.; Ess, D. H.; McCafferty, D. G.; Meyer, T. J. Proton-coupled Electron Transfer. *Chem. Rev.* **2012**, *112*, 4016–4093.

(43) Montalti, M.; Credi, A.; Prodi, L.; Gandolfi, M. T. *Handbook of Photochemistry*; CRC press: Boca Raton , FL, 2006; p 87.

(44) Rubio-Pons, Ò.; Serrano-Andrés, L.; Merchán, M. A Theoretical Insight into the Photophysics of Acridine. *J. Phys. Chem. A.* **2001**, *105*, 9664–9673.

(45) Wilkinson, F.; Helman, W. P.; Ross, A .B. Quantum Yields for the Photosensitized Formation of the Lowest Electronically Excited Singlet State of Molecular Oxygen in Solution. *J. Phys. Chem. Ref. Data* **1993**, *22*, 113–262.

(46) (a) Kasama, K.; Kikuchi, K.; Yamamoto, S.; Ujiie, K.; Nishida, Y.; Kokubun, H. Relaxation Mechanism of Excited Acridine in Nonreactive Solvents. *J. Phys. Chem.* **1981**, *85*, 1291–1296. (b) Kikuchi, K.; Kasama, K.; Kanemoto, A.; Ujiie, K.; Kikubun, H. Reaction and Deactivation of Excited Acridine in Ethanol. *J. Phys. Chem.* **1985**, *89*, 868–871. (c) Okada, K.; Okubo, K.; Oda, M. A Simple and Convenient Photodecarboxylation Method of Intact Carboxylic Acids in The Presence of Aza Aromatic Compounds. *J. Photochem. Photobiol. A: Chem.* **1991**, *57*, 265–277.

(47) Kumar, M.; Natarajan, E.; Neta, P. Electron Transfer and Alkyl Transfer with Cobaloximes in Aqueous Solutions. Kinetic Studies by Pulse Radiolysis. *J. Phys. Chem.* **1994**, *98*, 8024–8029.

(48) Kira, A.; Kato, S.; Koizumu, M. Studies of the Photoreduction of Acridine in Ethanol by the Flash Technique. *Bull. Chem. Soc. Jpn.* **1966**, *39*, 1221−1227.

(49) (a) Ohashi, Y. Dynamic Motion and Various Reaction Paths of Cobaloxime Complexes in Crystalline-state Photoreaction. *Crystallogr. Rev.* **2013**, *19*, 2−146. (b) Rangel, M.; Arcos, T.; de Castro, B. Photolysis Primary Products of Alkylcobaloximes Controlled by the Cobalt−Carbon Bond Strength. *Organometallics* **1999**, *18*, 3451−3456.

(50) Jothivenkatachalam, K.; Mohan, S. C. Photolytic Cleavage of Co–C Bond: A Mechanistic Study for the Formation of Solvent Coordinated Cobalt(II) Complex. *J. Organomet. Chem.* **2014**, *749*, 61–68.

(51) Ng, F. T.; Rempel, G. L.; Mancuso, C.; Halpern, J. Decomposition of α-Phenethylbis(dimethylglyoximato)cobalt(III) Complexes. Influence of Electronic and Steric Factors on the Kinetics and Thermodynamics of Cobalt−Carbon Bond Dissociation. *Organometallics* **1990**, *9*, 2762–2772.

(52) Edge, D. J.; Kochi, J. K. Electron Spin Resonance Studies of Carboxy Radicals. Adducts to Alkenes. *J. Am. Chem. Soc.* **1973**, *95*, 2635–2643.

(53) Experimental studies indicate that the reaction proceeds at near diffusion-controlled rates, pointing to a barrierless or a very low barrier process.[31b]

(54) (a) Jacques, P. A.; Artero, V.; Pécaut, J.; Fontecave, M. Cobalt and Nickel Diimine-Dioxime Complexes as Molecular Electrocatalysts for Hydrogen Evolution with Low Overvoltages. *Proc. Natl. Acad. Sci. U.S.A.* **2009**, *106*, 20627–20632. (b) Dempsey, J. L.; Winkler, J. R.; Gray, H. B. Mechanism of H_2 Evolution from a Photogenerated Hydridocobaloxime. *J. Am. Chem. Soc.* **2010**, *132*, 16774–16776. (c) Bhattacharjee, A.; Andreiadis, E. S.; Chavarot-Kerlidou, M.; Fontecave, M.; Field, M. J.; Artero, V. A Computational Study of the Mechanism of Hydrogen Evolution by Cobalt(diimine-dioxime) Catalysts. *Chem. Eur. J.* **2013**, *19*, 15166–15174. (d) Solis, B. H.; Yu, Y.; Hammes-Schiffer, S. Effects of Ligand Modification and Protonation on Metal Oxime Hydrogen Evolution Electrocatalysts. *Inorg. Chem.* **2013**, *52*, 6994–6999. (e) Lacy, D. C.; Roberts, G. M.; Peters, J. C. The Cobalt Hydride That Never Was: Revisiting Schrauzer's " Hydridocobaloxime". *J. Am. Chem. Soc.* **2015**, *137*, 4860–4864.

TOC graphic